Bortezomib induces apoptosis in esophageal squamous cell carcinoma cells through activation of the p38 mitogen-activated protein kinase pathway

Mercedes Lioni,[1] Kazuhiro Noma,[1]
Andrew Snyder,[1] Andres Klein-Szanto,[2]
J. Alan Diehl,[3] Anil K. Rustgi,[4] Meenhard Herlyn,[1]
and Keiran S.M. Smalley[1]

[1]The Wistar Institute; [2]Fox Chase Cancer Center; [3]Department of Cancer Biology, Abramson Family Cancer Research Institute; and [4]Gastroenterology Division, Department of Medicine, Department of Genetics, Abramson Cancer Center, University of Pennsylvania School of Medicine, Philadelphia, Pennsylvania

Abstract

Esophageal squamous cell carcinoma (ESCC) is an exceptionally drug-resistant tumor with a 5-year survival rate <5%. From an initial drug screen, we identified bortezomib as having robust activity in ESCC lines. Mechanistically, bortezomib induced a G_2-M-phase cell cycle arrest and p53-independent apoptosis associated with caspase cleavage and Noxa induction. Bortezomib also showed excellent activity in organotypic culture and *in vivo* models of ESCC. Biochemically, bortezomib treatment activated the p38 and c-Jun NH_2-termnial kinase stress-activated mitogen-activated protein kinase (MAPK) pathways and induced phospho-H2AX activity. Although H2AX is known to cooperate with c-Jun NH_2-termnial kinase to induce apoptosis following UV irradiation, knockdown of H2AX did not abrogate bortezomib-induced apoptosis. Instead, blockade of p38 MAPK signaling, using either small interfering RNA or a pharmacologic inhibitor, reversed bortezomib-induced apoptosis and the up-regulation of Noxa. Radiation therapy is known to activate the p38 MAPK pathway and is a mainstay of ESCC treatment strategies. In a final series of studies, we showed that the coadministration of bortezomib with irradiation led to enhanced p38 MAPK activity and a significant reduction in colony formation. We therefore suggest that p38 MAPK pathway activation is an excellent potential therapeutic strategy in ESCC. It is further suggested that bortezomib could be added to existing ESCC therapeutic regimens. [Mol Cancer Ther 2008;7(9):2866–75]

doi:10.1158/1535-7163.MCT-08-0391

Introduction

Esophageal cancers are among the most aggressive tumors known with over 75% of newly diagnosed patients dying within the first year. Five-year survival rates are also dismal (5-10%), with over 50% of patients harboring distant metastases at the time of presentation (1). One source for optimism is the current revolution in molecularly targeted cancer therapy. Recently, there has been a great deal of progress in the identification of key "driver" oncogenic mutations and signaling pathway activities that can be targeted by small-molecule pharmacologic inhibitors. In particular, striking results have been observed with imatinib (Gleevec) in chronic myeloid leukemia and gastrointestinal stromal tumors and gefitinib (Iressa) and erlotinib (Tarceva) in non-small cell lung carcinoma (2–5). To date, such "targeted" strategies have been not been explored extensively in esophageal squamous cell carcinoma (ESCC). As tumors often posses multiple genetic and cell signaling lesions, the inhibition of one signaling pathway is often therapeutically ineffective (6). Rather, more success can be envisioned with agents targeted against multiple cellular pathways. One such multipathway inhibitor is the novel proteasome inhibitor bortezomib (Velcade). Bortezomib is a dipeptidyl boronic acid that inhibits the 26S proteasome, a large multisubunit protein complex that degrades polyubiquitinated target proteins, such as the cyclins, apoptosis regulators, and p53 (7, 8). Although the proteasome performs many important housekeeping functions in normal cells, the increased metabolic activity and rapid cycling seen in transformed cells makes proteasome function critical for tumor cell survival (7). The mechanisms of bortezomib-induced cell death remain poorly defined and appear to be cell type specific or context dependent. In melanoma and head and neck carcinoma cell lines, increased Noxa expression appears to be critical for apoptosis induction (9, 10).There is also evidence that the generation of cellular stress leading to reactive oxygen species (ROS) is a critical feature of the anticancer activity of bortezomib (11). In the current study, we show that bortezomib is strongly apoptotic in ESCC lines and blocks the growth and survival of these cells in three-dimensional organotypic cultures and animal xenograft models, thereby providing complementary *in vitro* and *in vivo* findings. We further show that bortezomib exerts its proapoptotic effects through a novel mechanism involving the activation of the p38 mitogen-activated protein kinase (MAPK) pathway.

Materials and Methods

Cell Lines

Esophageal cancer cells, TE cell lines (TE1, TE3, TE8, TE10, TE11, and TE12), and FEF3 (fetal esophageal fibroblasts) are available commercially and through the NIH/National Institute of Diabetes Digestive and Kidney Diseases Center for Molecular Studies in the Digestive and Liver Diseases' Cell Culture Core Facility (University of Pennsylvania) and were cultured as described previously (12). Human microvascular endothelial cells (HMVEC) are available commercially through Cascade Biologics and were cultured as described previously (13).

Antibodies and Reagents

H2AX, phospho-H2AX, p53, p21, and Noxa antibodies were purchased from Calbiochem. p38 MAPK, phospho-p38 MAPK, caspase-3, and poly(ADP-ribose) polymerase (PARP) antibodies were purchased from Cell Signaling. Mouse monoclonal anti-human CD31 antibody was purchased from DAKO North America. Texas red-conjugated anti-phalloidin antibody was purchased from Molecular Probes. Texas red-conjugated anti-mouse secondary antibody and fluorescein-conjugated anti-rabbit secondary antibody were from Vector Laboratories. TUNEL, *In situ* Cell Death Detection Kit, was used from Boehringer Mannheim/Roche. Ki-67 staining was done using Ki-67 antibody from Abcam. For *in vitro* assays, stock solutions (10 mmol/L) of the c-Jun NH_2-termnial kinase (JNK) inhibitor VIII (Calbiochem), proteasome inhibitor-1 (Calbiochem), MG-132 (Calbiochem), and SB230580 (Calbiochem) were prepared in DMSO and stored at -20°C. Stock solutions of 1 μmol/L bortezomib (Millennium Pharmaceuticals) were prepared in normal saline and stored at -20°C. Stock solutions of 10 μmol/L z-VAD-FMK (Sigma) were prepared in DMSO and stored at -20°C.

In vitro Three-Dimensional Network Formation Assay and Fluorescence Imaging

Reconstruction of vessel-like structure in three-dimensional collagen gels and subsequent fluorescent staining of networks/cords in whole-mount gels were done as described previously (13).

Western Blotting Analysis

Experiments were done as described previously (6).

Irradiation Experiments

Genotoxic stress was induced by exposing the U2OS cells to ionizing radiation at a dose of 3 Gy for a 3 min period (IR; J.L. Shepherd Mark 1 Model 30, [137]Ce Irradiator; J.L. Shepherd and Associates). TE12 cells were plated in four groups (control, control irradiated, bortezomib alone, and bortezomib + radiation) at 30 or 60 cells per well in 96-well plates (n = 6). Bortezomib-treated plates received 10 nmol/L of drug for 4 h before irradiation. The radiation plates received 2 Gy radiation. Plates were examined for the presence of colonies after 2 weeks, and the number of colonies per well was scored.

Transfection

To achieve transient suppression of gene expression of H2AX and p38 MAPK, Dharmacon *SMART* pool small interfering RNAs (siRNA) were used as described previously (12).

Organotypic Cell Culture

Reconstructs of human ESCC were grown as described (12, 14).

Immunofluorescence Microscopy

TE12 cells were seeded onto glass coverslips in six-well plates and incubated overnight. Cells were then fixed and analyzed as described previously (12) Immunofluorescence detection of Ki-67 and TUNEL on the esophageal reconstructs were done as described (15).

Generation of ROS

TE12 cells were treated with 500 μmol/L H_2O_2 for 1 h, 10 nmol/L bortezomib for 24 h, and normal saline 24 h. The cells were trypsinized and incubated with 100 nmol/L CM-H_2DCFDA (Invitrogen) before being washed and resuspended in PBS. Cellular ROS was measured by flow cytometry. Data shown are representative of three independent experiments.

Adherent Cell Proliferation Assay

Cells were plated into a 96-well plate at a density of 2.5×10^4/mL and left to grow overnight. Inhibition of proliferation was analyzed by the MTT assay as described previously (6).

Cell Cycle Analysis

Cell cycle analysis was done after treatment with bortezomib 10 nmol/L (0, 8, 24, and 48 h) as described (6).

Three-Dimensional Spheroid Growth

Esophageal carcinoma spheroids were prepared using the liquid overlay method as described (6).

In vivo experiments

The study protocol was approved by the Wistar Institute Animal Care and Use Committee. Each group consisted of eight NOD/SCID mice. Sixteen mice were injected s.c. with TE11 cells (2×10^6) into the lower back. When animals developed nodules of about 5 mm in diameter, the study drug administration was initiated (day1). The NOD/SCID mice were assigned randomly to two experimental groups of eight animals each: (*a*) 200 μL normal saline and (*b*) 1 mg/kg bortezomib (in 200 μL normal saline) by i.p. injection twice a week. The dose chosen in the present study were based on preliminary dose-finding experiments. During the experiment, tumor volumes were assessed twice weekly by caliper measurements. At treatment day 16, 6 h after the final drug application, all animals were euthanized. Data show the mean ± SE of the treated and untreated groups from one experiment.

Results

Bortezomib Inhibits the Proliferation of Human ESCC Cell Lines through G_2-M Cell Cycle Arrest and Induction of Apoptosis

As targeted therapeutic approaches have not been attempted in ESCC in an extensive fashion, we initiated our studies by screening a panel of ESCC lines against

inhibitors of MEK (U0126), PI3K (LY294002), glycogen synthase kinase-3β (DW1/2; ref. 16), the proteasome (MG-132, proteasome inhibitor-1, and bortezomib), Hedgehog (cyclopamine), and cyclooxygenase-2 (NS-398) (Supplementary Table S1).[5] In our initial screen, compounds were tested both in a two-dimensional cell culture assay (MTT) and in a three-dimensional collagen implanted spheroid assay (6). Two-dimensional and three-dimensional models were used as the pharmacologic profiles of drugs in two-dimensional cell culture are not predictive of response in three-dimensional cell culture or *in vivo* (6). Of the compounds tested, only the proteasome inhibitors MG-132, proteasome inhibitor-1, and bortezomib continued to show good anticancer activity under both model systems (Fig. 1; Supplementary Fig. S1).[5]

Treatment of six human ESCC lines (TE1, TE3, TE8, TE10, TE11, and TE12) with increasing concentrations of bortezomib (1 nmol/L-10 μmol/L) led to a concentration-dependent decrease in cell growth (Fig. 1A). Cell cycle analysis on the TE12 cell line showed that treatment with bortezomib (10 nmol/L) led to a time-dependent (0, 8, 24, and 48 h) increase in the G_2-M, S, and sub-G_1 phases of the cell cycle (Fig. 1B). The increase in the sub-G_1 population following bortezomib treatment was indicative of the cells undergoing apoptosis. Similar proapoptotic effects were also noted in the TE1, TE3, and TE10 cell lines (Supplementary Fig. S1A).[5] Bortezomib was also highly effective in our three-dimensional spheroid model and reduced both the cell viability (as witnessed by loss of green staining and increased red fluorescence) and invasion of the TE12 line in a concentration-dependent manner (Fig. 1C). Other proteasome inhibitors (proteasome inhibitor-1 and MG-132) were also found to have similar effects on the invasion and survival of two other ESCC lines (TE1 and TE10) in our spheroid model (Supplementary Fig. S1B;[5] not shown).

Treatment of TE12 cells with bortezomib (10 nmol/L) induced the rapid (<12 h) cleavage of caspase-3 and PARP (Fig. 1D). Similar caspase-3 and PARP cleavage was also seen in TE1 cells treated with the proteasome inhibitor MG-132 (Supplementary Fig. S1C).[5] As the TE12 cell line has mutated p53 (17), we did not observe any increase in the expression of p53 or its downstream target p21 following bortezomib administration. However, both p53 and p21 expression was increased in 1205Lu cells, a melanoma cell line that retains functional p53 (16). The proapoptotic protein Noxa was shown to be rapidly up-regulated (<8 h) in both the TE12 ESCC line and the 1205Lu melanoma line (Fig. 1D). There is some suggestion that increased Noxa expression is a consequence of ROS generation. To investigate this, we treated the TE12 cell line with bortezomib and measured the increase in fluorescence of the cell-permeable ROS probe CM-H$_2$DCFDA (Supplementary Fig. S2).[5] It was found that, although the positive

control (hydrogen peroxide) induced a rightward shift in the curve, there was no equivalent increase in fluorescence intensity seen following bortezomib treatment, indicating that this was not inducing apoptosis through ROS generation (Supplementary Fig. S2).[5]

Bortezomib Induces Apoptosis in a Three-Dimensional Organotypic Model of ESCC and Inhibits Angiogenesis

We next tested bortezomib in two more elaborate ESCC models that allowed us to assess its effects on both stromal fibroblasts and endothelial cells. In the first model, ESCC were layered on top of a tissue-like matrix consisting of esophageal fibroblasts and collagen. Here, we found that treatment with bortezomib (500 nmol/L or 1 μmol/L) led to a concentration-dependent increase in the level of apoptosis as seen by the enhanced TUNEL staining (Fig. 2A and B). Interestingly, the effects of the bortezomib were relatively tumor cell specific, and there was little positive TUNEL staining seen in the underlying fibroblast layer.

Many targeted therapies also have unintended beneficial effects on angiogenesis. To investigate this, we used a model where the interaction of ESCC and human esophageal fibroblasts cooperate to induce vascular network formation of HMVEC. In control cultures, the interaction of ESCC and fibroblasts induced the HMVEC to lift off the bottom of the plate and grow upwards into the acellular collagen layer, where they formed organized vascular networks, as shown by the increased CD31 staining (Fig. 2C). Treatment of the cultures with bortezomib (0.5 μmol/L) completely inhibited the organized vascular network formation, and only a sparse layer of unorganized HMVEC was observed (Fig. 2C).

Bortezomib Induces Regression of Established Human ESCC Xenografts through Inhibition of Proliferation and Apoptosis Induction

Next, we grew TE11 cells as tumor xenografts in NOD/SCID mice. After tumor establishment (5 × 5 mm), mice were dosed twice weekly with 1 mg/kg bortezomib by i.p. injection. After 14 days, it was found that bortezomib treatment had significantly suppressed tumor growth (vehicle treated: 4.2 ± 0.2-fold; bortezomib treated: 0.6 ± 0.1-fold) and led to significant ($P < 0.05$) tumor regression (Fig. 3A and B). To assess the mechanism of action of bortezomib in the xenografts, sections were taken from control and treated tumors and stained for either proliferation (Ki-67) or apoptosis induction (TUNEL; Fig. 3C). It was noted that 14-day bortezomib treatment led to a significant ($P < 0.05$) reduction in Ki-67 positivity while concurrently increasing TUNEL staining (Fig. 3D).

Treatment of ESCC Lines with Bortezomib Induces Phospho-H2AX Foci Downstream of Caspase-3 Activation

It is known that, during the DNA damage response, activated H2AX localizes to discrete nuclear foci at the site of DNA double-strand breaks. Treatment of the TE12 cells with bortezomib (10 nmol/L) caused a massive up-regulation of phospho-H2AX in the nucleus, with high-power magnification revealing the discrete focal expression of the H2AX (Fig. 4A, *inset*). As recent studies have shown

---

[5] Supplementary material for this article is available at Molecular Cancer Therapeutics Online (http://mct.aacrjournals.org/).
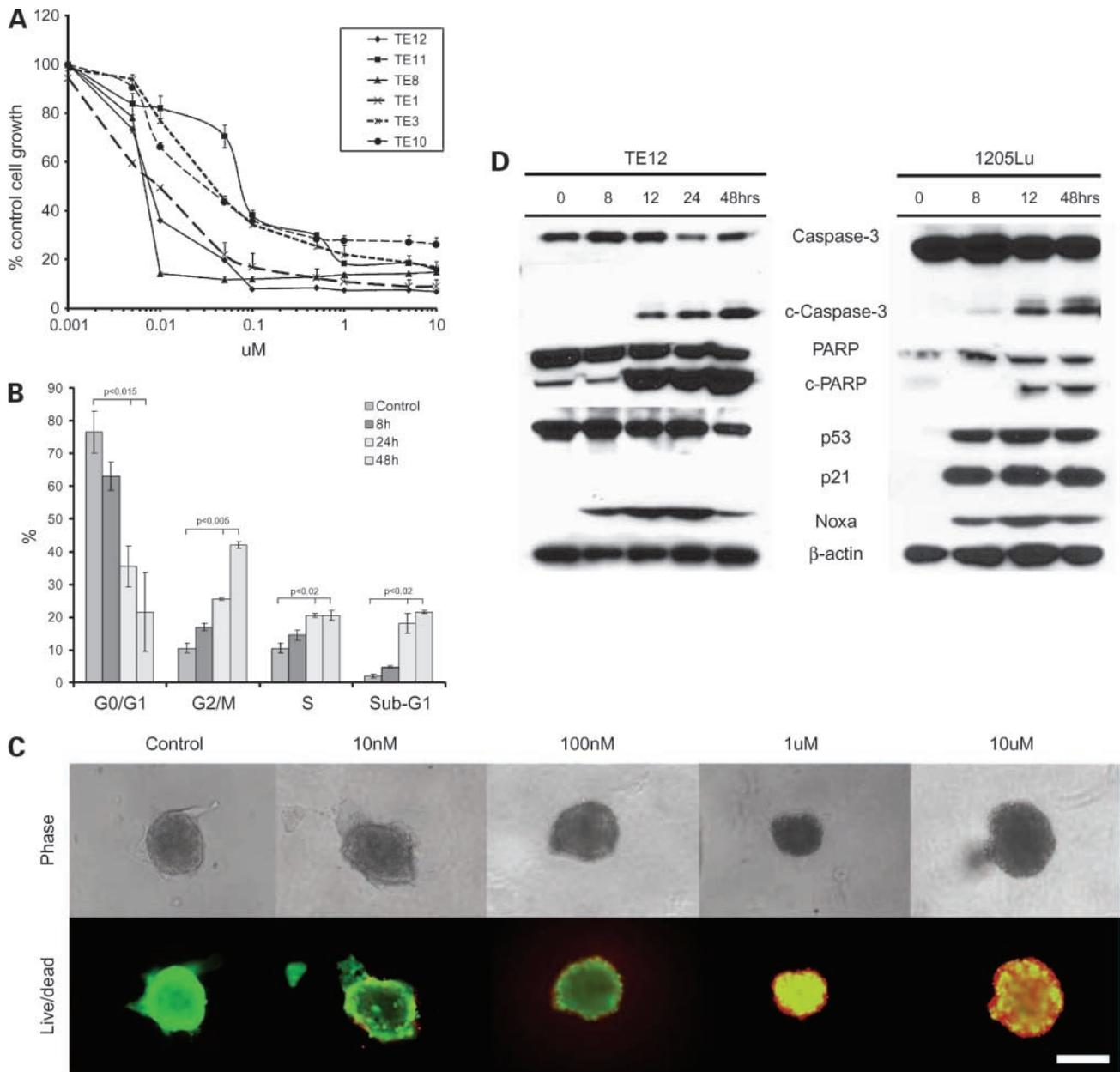
Figure 1. Bortezomib inhibits the proliferation of human ESCC cell lines through G_2-M cell cycle arrest and induction of apoptosis. **A,** in two-dimensional adherent cell culture, bortezomib reduces growth of the ESCC cell lines in a concentration-dependent fashion. Adherent TE1, TE3, TE8, TE10, TE11, and TE12 cells were treated with increasing concentrations of bortezomib (1 nmol/L-10 μmol/L) for 72 h before being treated with MTT. The resulting changes in absorbance were read in a plate reader at 490 nm and expressed as a percentage of control absorbance. Mean ± SE of three independent experiments. **B,** inhibition of cell growth by bortezomib is associated with G_2-M cell cycle arrest. Adherent TE12 cells were treated with saline or 10 nmol/L bortezomib for 8, 24, or 48 h. Cells treated with bortezomib were found to enter G_2-M phase cell cycle arrest with increasing periods. The cell cycle profile was obtained using 15,000 cells. Mean ± SE of three independent experiments. **C,** bortezomib blocks growth of TE cells in three-dimensional culture. TE12 cells were grown under nonadherent conditions for 72 h until spheroids had formed. Spheroids were then harvested and embedded into a collagen matrix before being treated with normal saline or bortezomib (10 nmol/L-10 μmol/L). After 72 h, spheroids were treated with calcein-AM (viable cells; *green*) and ethidium bromide (dead cells; *red*). Representative of three independent experiments. Magnification, ×4. Bar, 100 μm. **D,** Western blot showing induction of apoptosis in cells treated with bortezomib. TE12 (ESCC) and 1205Lu (melanoma) cells were treated with 10 nmol/L bortezomib for increasing periods (0-48 h) followed by protein extraction and probing for expression of cleaved caspase-3/PARP, p53, p21, and Noxa. β-Actin is shown as a loading control.

that H2AX activation may play an important role in apoptosis induction (18), we transfected TE12 cells with a siRNA against H2AX, which led to near-total protein knockdown after 4 days of treatment (Fig. 4B). Any possible role of H2AX in bortezomib-induced apoptosis induction was discounted by the fact that protein knockdown did not reduce either caspase-3 cleavage or DNA laddering (Fig. 4C; data not shown). Next, we investigated whether

the increase in phospho-H2AX occurred as a downstream consequence of DNA strand breaks following caspase cleavage. In these studies, the TE12 cells were pretreated using the pan-caspase inhibitor z-VAD-FMK (1 μmol/L) before bortezomib treatment. Here, the inhibition of bortezomib-induced caspase activation completely blocked the phosphorylation of H2AX, indicating that this occurred following caspase cleavage (Fig. 4D).

p38 MAPK Activity Is Critical to Bortezomib-Induced Apoptosis and Interaction with Radiation Treatment

Previous work has shown that p38 MAPK is critical for radiation-induced G_2-M arrest (19). As bortezomib induces a G_2-M cell cycle arrest in the ESCC lines (Fig. 1B), the potential role of p38 MAPK in the activity of bortezomib was addressed. Treatment of the cells with bortezomib (10 nmol/L) induced the phosphorylation (<4 h) of p38
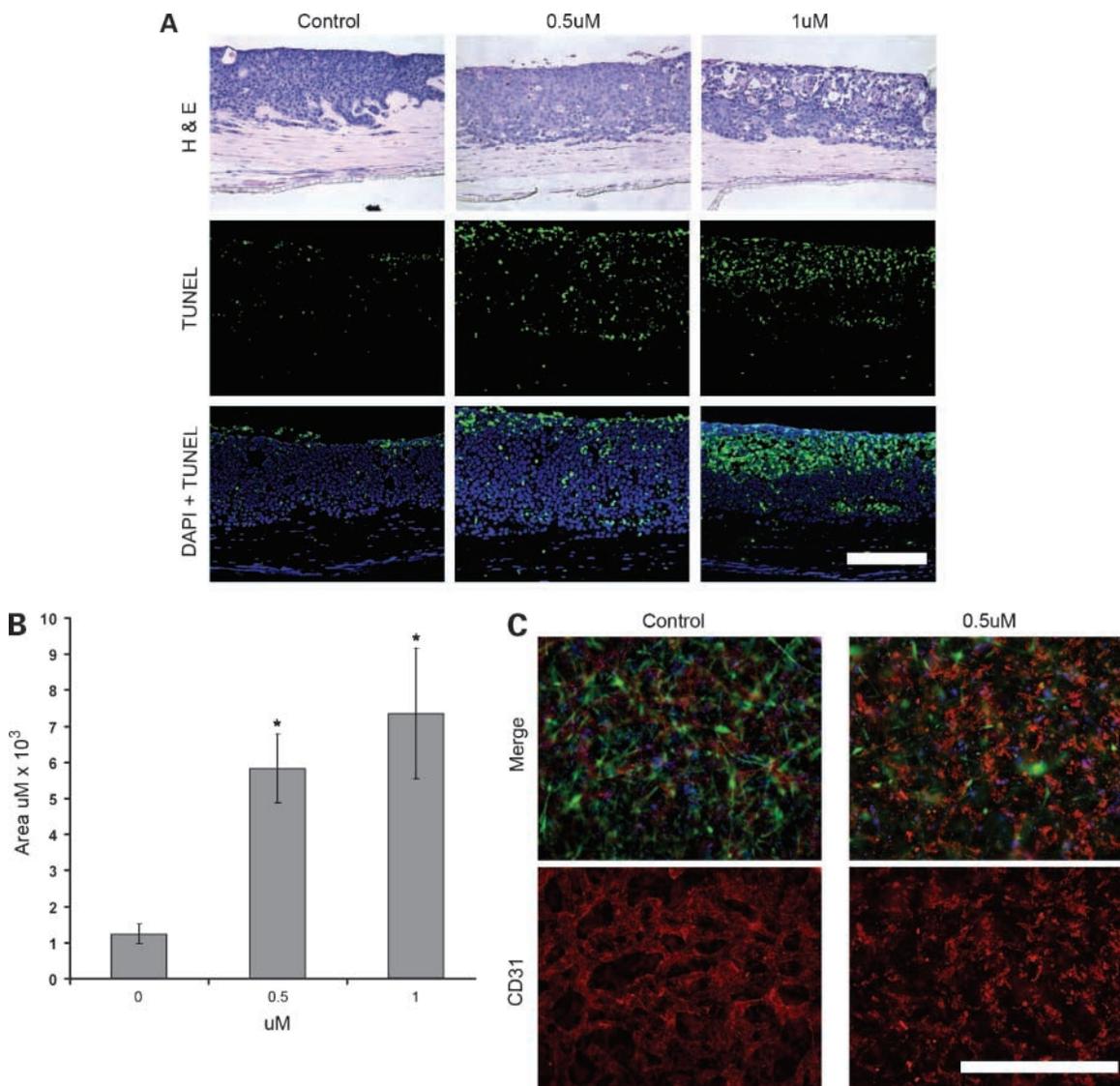

Figure 2. Bortezomib induces apoptosis in a three-dimensional organotypic model of ESCC and inhibits vascular network formation. **A,** three-dimensional organotypic cultures were formed in a Transwell system using a collagen and fibroblast matrix on the bottom and ESCC (TE12 cells) seeded on top. After 14 d, the cultures were treated with bortezomib (0, 0.5, and 1 μmol/L). After 72 h, the reconstructs were harvested and paraffin-embedded. TUNEL staining was carried out to quantify apoptotic cells after treatment. *Green,* TUNEL; *blue,* DAPI. Magnification, ×10. Bar, 100 μm. **B,** quantification of apoptotic TE12 cells in treated reconstructs (as shown in **A**). Total area of positive TUNEL staining (μmol/L × 10³) was assessed using ProImage 6.0 software. Representative of three independent experiments. *, $P < 0.05$. **C,** vascular networks were created using HMVEC that were cultured and overlaid with collagen I followed by a second overlay of collagen containing TE12 cells and esophageal fibroblasts (FEF3). After solidification of the collagen matrix, cells were treated with 0 (normal saline) or 0.5 μmol/L bortezomib for 72 h. Three-dimensional angiogenesis models were harvested and immunofluorescence staining was done, showing green fluorescent protein-tagged FEF3 esophageal fibroblasts (*green*), HMVEC (CD31; *red*), and total nuclei (DAPI; *blue*). All representative images are shown as a three-color merge, with the monochrome images of CD31 staining. Bortezomib treated three-dimensional angiogenesis model showed decreased vascular network formation in comparison with the control. Magnification, ×20. Bar, 100 μm.
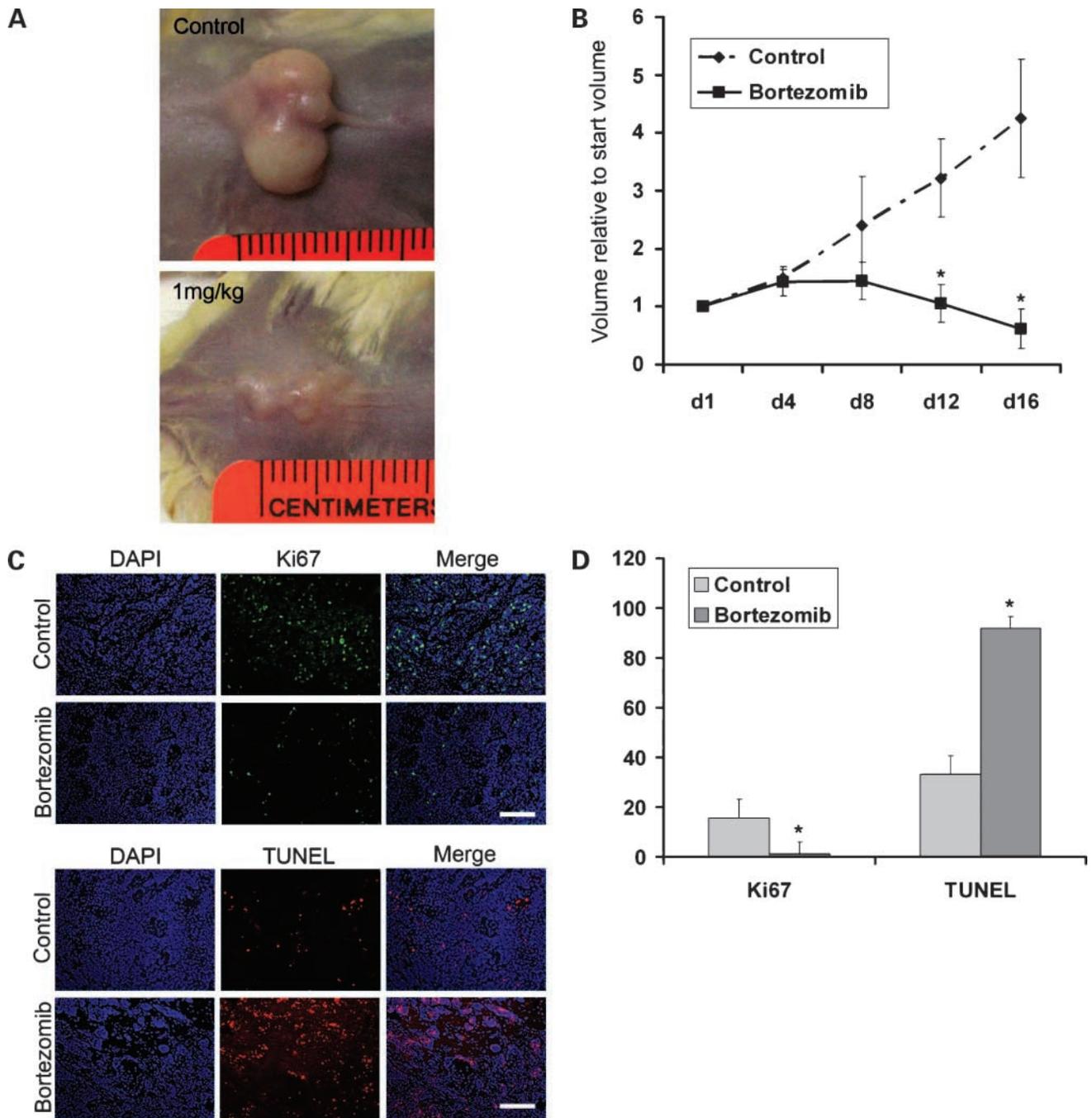
Figure 3. Bortezomib induces regression of established human ESCC xenografts through inhibition of proliferation and apoptosis induction TE11 cells were grown as tumor xenografts in NOD/SCID mice. After tumor establishment, mice were dosed twice weekly with 0 (normal saline) or 1 mg/kg bortezomib i.p. (8 mice per group) for 16 days. **A,** photographs of representative tumors for each group at day 16. **B,** growth curves normalized to the start volumes. Bortezomib treatment led to significant (*, $P < 0.05$) levels of tumor regression. **C,** immunofluorescent staining of tumors from each group. TUNEL and Ki-67 staining was done in paraffin-embedded sections [TUNEL (*red*), Ki-67 (*green*), and DAPI (*blue*)]. Magnification, ×10. Bar, 50 μm. **D,** quantification of immunofluorescence for treated and untreated tumors. Percentage of positive cells in each group. *, $P < 0.04$.

MAPK (Fig. 5A). A critical role for p38 MAPK in bortezomib-induced apoptotic response was shown by the ability of the specific p38 MAPK inhibitor SB230580 (10 μmol/L) to block caspase-3 cleavage (Fig. 5B). Pretreatment of the cells with SB230580 also blocked the bortezomib-induced activation of both Noxa and phospho-H2AX (Fig. 5B), showing that p38 MAPK is a critical pathway necessary for the anticancer activity of bortezomib in ESCC lines. We further showed that knockdown of p38 MAPKα protein expression using a siRNA was similarly able to

block bortezomib-induced caspase cleavage (Fig. 5C). Next, it was shown that bortezomib also activated another stress-activated MAPK, the JNK pathway (Supplementary Fig. S3). However, unlike p38 MAPK, there was little evidence for this pathway being directly involved in bortezomib-induced apoptosis, as inhibition of the pathway, using the small-molecule inhibitor JNK inhibitor VIII (1 μmol/L), did not attenuate the level of bortezomib-induced caspase-3 cleavage.

It is known that irradiation activates the p38 MAPK pathway. Given that preoperative radiotherapy is a standard treatment for ESCC, we next explored whether there was any positive interaction between bortezomib and irradiation. Treatment of the TE12 cells with either bortezomib (10 nmol/L) or radiation (2 Gy) led to a modest increase in p38 MAPK activity (Fig. 5D), whereas coadministration of the drug with irradiation significantly increased the level of p38 MAPK activity. The enhanced p38 MAPK activity also translated into increased cytotoxicity with the administration of bortezomib (4 h, 10 nmol/L) before irradiation (2 Gy), significantly ($P < 0.0001$) reducing the formation of TE12 colonies over a 14-day period (Fig. 5D).

Discussion

In the current study, we describe the possible therapeutic utility of the proteasome inhibitor bortezomib in ESCC and elucidate a completely novel mechanism of action for this drug involving p38 MAPK-dependent apoptosis. In our initial screen, it was noted that only proteasome inhibitor-1/MG-132/bortezomib had good anticancer activity in both two-dimensional and three-dimensional models.
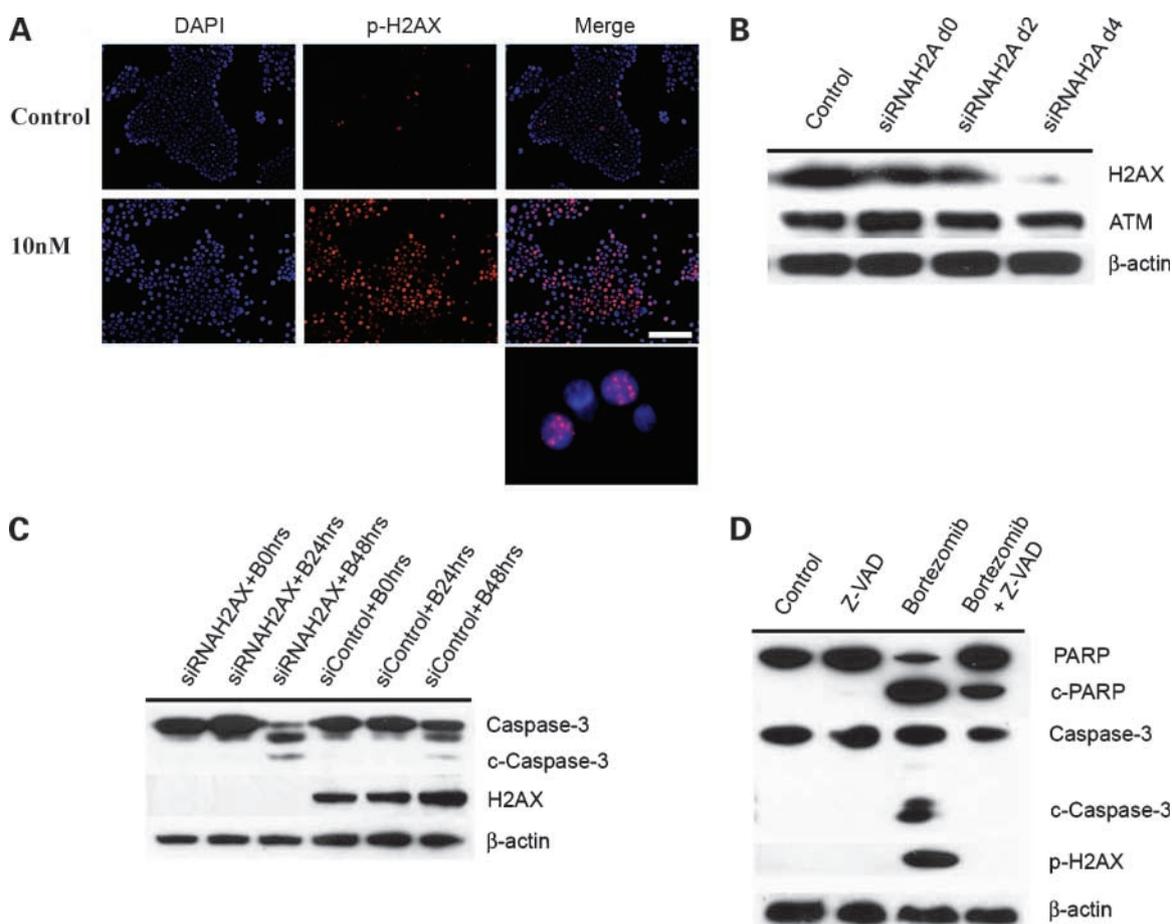

Figure 4. Knockdown of H2AX expression does not inhibit bortezomib-induced apoptosis. **A,** immunofluorescence showing γ-H2AX foci formation after bortezomib treatment. TE12 cells were grown on glass slides and treated with normal saline or 10 nmol/L bortezomib for 12 h. Slides were harvested, fixed, and permeabilized before being stained for phospho-H2AX [γ-H2AX (*red*) and DAPI (*blue*)]. Magnification, ×20. Bar, 50 μm. *Inset,* magnification, ×60. Bar, 50 μm. **B,** Western blot showing the down-regulation of H2AX after day 4 of siRNA transfection. Proteins were extracted and resolved followed by probing for H2AX, ATM, and β-actin. **C,** H2AX knockdown TE12 cells and control cells were treated with 10 nmol/L bortezomib for 24 and 48 h. Cells were harvested, lysed, and probed for caspase-3 cleavage. No difference in caspase-3 cleavage was observed in H2AX knockdown cells compared with control cells. **D,** TE12 cells were treated with z-VAD-FMK (1 μmol/L), bortezomib, or a combination of both for 48 h. Cells lysates were then harvested, resolved by Western blotting, and probed for cleaved-PARP (*c-PARP*), cleaved caspase-3 (*c-Caspase-3*), total caspase-3 (*Caspase-3*), total PARP (*PARP*), and phospho-H2AX (*p-H2AX*). Equal protein loading was confirmed by stripping of the blot and reprobing for actin expression.
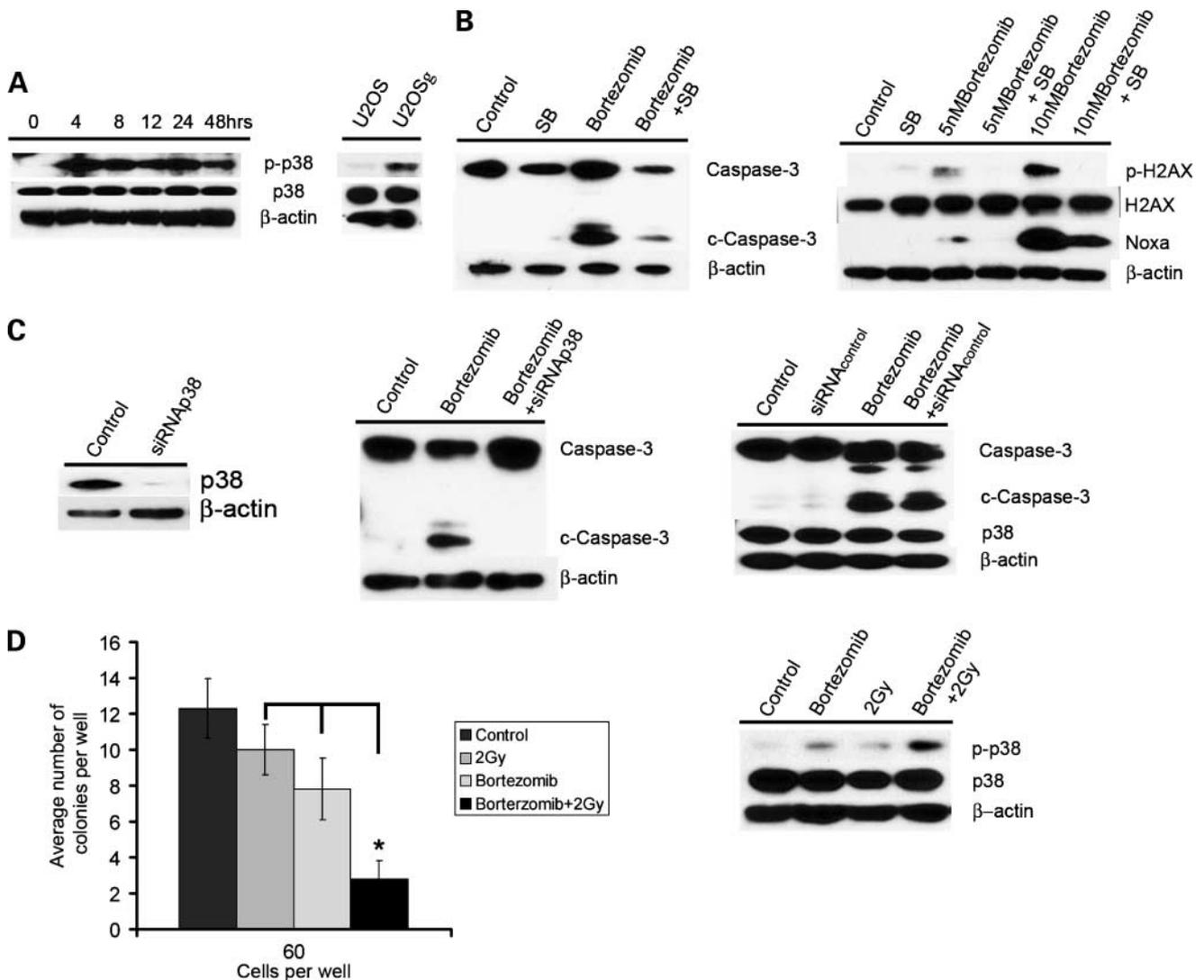
Figure 5. p38 MAPK activity is critical to bortezomib-induced apoptosis and interaction with radiation treatment. **A,** bortezomib treatment led to the rapid up-regulation of phospho-p38 MAPK (*p-p38*) activity in TE12 cells. Irradiation of the human osteosarcoma line U2OS also led to the rapid up-regulation of p38 activity. Equal protein expression was confirmed by stripping and probing the blot for actin expression. **B,** inhibition of p38 MAPK reverses bortezomib-induced apoptosis. TE12 cells were pretreated with 10 μmol/L SB230580 for 24 h before being treated with bortezomib (10 nmol/L) for 48 h. Cells were harvested, lysed, and probed for caspase-3 cleavage, total caspase-3, phospho-H2AX, total H2AX, and Noxa expression. Equal protein loading was confirmed by stripping the blot and probing for actin expression. **C,** knockdown of p38 MAPK inhibits bortezomib-induced caspase-3 cleavage. TE12 cells were transiently transfected using *SMART*pool siRNA p38 MAPK (*siRNAp38*). Control cells were transfected with a scrambled siRNA sequence (*siRNAcontrol*) After 4 days, cells were treated with bortezomib (10 nmol/L, 48 h). Protein was then extracted from the cells, resolved, and probed for expression of caspase-3, cleaved caspase-3 (*c-caspase-3*), and total p38 MAPK (*p38*). **D,** Western blot showing the positive interaction of bortezomib and radiation in the activation of p38 MAPK signaling. TE12 cells plated in 10 cm dishes were treated with control, 2 Gy radiation alone, bortezomib alone, and bortezomib + radiation (2 Gy). Plates were pretreated for 4 h with saline or bortezomib (10 nmol/L) before irradiation. Cells were left to grow overnight before the extraction of protein; extracts were then resolved and probed for expression of phospho-p38 MAPK, total p38 MAPK, and β-actin. Radiation survival. Cells were plated in 96-well plates at the indicated number per well. Cells were then treated with either saline (control) or bortezomib (10 nmol/L) for 4 h before radiation. Cells were left to grow for 2 weeks, after this time the total number of colonies were counted. *Columns,* mean of six experiments. *, $P < 0.0001$.

Bortezomib was antiproliferative and strongly proapoptotic in two-dimensional ESCC cell cultures, three-dimensional organotypic cultures, and a human ESCC xenograft mouse model. The concentrations of bortezomib required to induce regression of established ESCC xenografts are lower than those reported for other solid tumors (20) and seem to

be readily achievable in the clinic (21). Unlike in other squamous cell carcinoma lines, such as PAM212, we did not find any effects on nuclear factor-κB signaling following bortezomib treatment (20). At least part of the potential activity of bortezomib against ESCC may be the result of impaired angiogenesis, as bortezomib was found

to inhibit tumor-induced vascular network formation in a three-dimensional model of ESCC-induced angiogenesis. It is however, difficult to conclude how bortezomib was exerting its antiangiogenic effects, particularly as the concentrations of bortezomib used were likely to induce apoptosis of the ESCC cells and may have in fact been the result of impaired ESCC/HMVEC interaction. Any potential antiangiogenic activity of bortezomib is likely to be of great significance to ESCC, as this is known to be a highly angiogenic tumor. Several studies have shown that angiogenesis, as measured by the extent of tumor microvessel density, as well as VEGF expression, are prognostic factors for ESCC (22–24). It was, however, difficult to confirm the bortezomib-driven inhibition of angiogenesis within our ESCC xenografts, as the tumors are typically not highly vascularized when grown in this model.

Treatment of human ESCC lines with bortezomib is strongly growth inhibitory, associated with induction of a G_2-M-phase cell cycle arrest and apoptosis. Induction of G_2-M arrest is typically associated with induction of p53 activity and transcription of its downstream target p21 (25). Previous studies have shown that almost all human ESCC lines have defects in p53 function, arising as a result of missense mutations in the coding sequence (17). In agreement with a lack of functional p53 in the ESCC lines, bortezomib was found to induce cleavage of caspase-3 and PARP without the induction of either p53 or its downstream target p21. In contrast, bortezomib did induce the activation of p53 and p21 in the 1205Lu melanoma cells (which are p53 wild-type). Bortezomib treatment was found to induce the rapid up-regulation of the proapoptotic protein Noxa in both the ESCC and the melanoma cell lines (10). Although Noxa is known to be a p53 target gene (26), the p53-independent induction of Noxa reported here is consistent with that observed in other studies using p53-mutated cancer cell lines (Jurkat, Sk-MEL-28, and MDA-MB-231; refs. 9, 10, 27).

Previous studies have shown that the induction of ROS can activate Noxa in response to bortezomib treatment and that this may be independent of p53 function (27). It has been also shown that ROS generation is associated with bortezomib activity in mantle cell lymphoma and small cell lung carcinoma (27, 28). Here, we found that bortezomib treatment was not associated with ROS generation. Instead, we observed an increase in the expression of phospho-H2AX, a marker of the DNA damage response. Recent work has shown that H2AX can mediate apoptosis directly where JNK directly phosphorylates H2AX leading to caspase-3 cleavage and caspase-activated DNase activity (18). As bortezomib both activates JNK signaling and induces H2AX phosphorylation, we next asked whether H2AX activity was required for bortezomib-induced apoptosis in ESCC lines. Although a siRNA against H2AX yielded good levels of protein knockdown, we did not observe any change in the magnitude of apoptosis induction or DNA laddering following 48 h bortezomib treatment, suggesting that the interaction of JNK and H2AX was not responsible for the apoptotic effects observed.

Another possible explanation for the observed DNA damage response involved the direct role of caspase activation in the cleavage of genomic DNA leading to subsequent H2AX/ATM activation. It was found that inhibition of caspase activity using z-VAD-FMK blocked the phosphorylation of H2AX, suggesting that the DNA damage response occurred following caspase cleavage.

Our initial studies showed activation of the G_2-M checkpoint following bortezomib treatment. UV irradiation is known to induce a G_2-M arrest through p38 MAPK-mediated inhibition of cdc25B activity (19). We next asked whether bortezomib activated the p38 MAPK pathway and whether this led to apoptosis in the ESCC cells. Bortezomib treatment was found to induce p38 MAPK activity and inhibition of p38 MAPK signaling, using an inhibitor or a siRNA, markedly inhibited bortezomib-induced caspase-3 cleavage. p38 MAPK activation was also required for the bortezomib-induced increase in Noxa expression and the phosphorylation of H2AX, as this could be also reversed by SB230580 treatment. Thus, it was shown that activation of p38 MAPK is a critical step for bortezomib-induced apoptosis in ESCC cells. Thus far, no direct link has been made between the activation of p38 MAPK and increased Noxa expression. Previously, it was shown that the p38 MAPK activated cofactor p18[HAMLET] increases Noxa expression following treatment with either UV or cisplatin (29). However, in this instance, Noxa is regulated through a p53-dependent mechanism. As our ESCC lines lack any functional p53 activity, this current study provides the first clues that p38 MAPK activity may regulate Noxa expression independently of p53.

The essential role for p38 MAPK in bortezomib-induced apoptosis in ESCC cells is in stark contrast to findings reported for multiple myeloma cells. Here, bortezomib also activates the p38 MAPK pathway but instead leads to drug resistance through increased expression of Hsp27 (30, 31). In multiple myeloma cells, it was shown that p38 MAPK pathway inhibition actually enhanced the proapoptotic effect of bortezomib through the down-regulation of Hsp27, Mcl-1, and Bcl-XL expression while up-regulating p53 activity (31, 32). Again, in contrast to our findings, this study also reported that increased JNK activity leads to enhanced caspase cleavage (31).

Preoperative radiotherapy is a front-line treatment for ESCC. As irradiation induces p38 MAPK, we investigated whether bortezomib-induced p38 activity would enhance responses to radiation treatment. Combined treatment of the ESCC cells with radiation and a single 4 h treatment with bortezomib enhanced both p38 MAPK activity and cytotoxicity in a colony formation assay. We therefore suggest that bortezomib treatment could be a potential radiosensitizing agent for ESCC. In summary, we have shown that bortezomib is a promising potential treatment for ESCC. We also found that bortezomib induces apoptosis in ESCC lines through a novel mechanism involving the p38 MAPK-induced Noxa activation, leading to caspase cleavage, which is depicted as a model in Supplementary Fig. S4.[5]

Disclosure of Potential Conflicts of Interest

References

1. Enzinger PC, Ilson DH, Kelsen DP. Chemotherapy in esophageal cancer. Semin Oncol 1999;26:12 – 20.

2. Sawyers C. Targeted cancer therapy. Nature 2004;432:294 – 7.

3. Druker BJ, Talpaz M, Resta DJ, et al. Efficacy and safety of a specific inhibitor of the BCR-ABL tyrosine kinase in chronic myeloid leukemia. N Engl J Med 2001;344:1031 – 7.

4. Pao W, Miller V, Zakowski M, et al. EGF receptor gene mutations are common in lung cancers from ''never smokers'' and are associated with sensitivity of tumors to gefitinib and erlotinib. Proc Natl Acad Sci U S A 2004;101:13306 – 11.

5. Lynch TJ, Bell DW, Sordella R, et al. Activating mutations in the epidermal growth factor receptor underlying responsiveness of non-small-cell lung cancer to gefitinib. N Engl J Med 2004;350:2129 – 39.

6. Smalley KS, Haass NK, Brafford PA, Lioni M, Flaherty KT, Herlyn M. Multiple signaling pathways must be targeted to overcome drug resistance in cell lines derived from melanoma metastases. Mol Cancer Ther 2006;5: 1136 – 44.

7. Adams J. The proteasome: a suitable antineoplastic target. Nat Rev Cancer 2004;4:349 – 60.

8. Adams J, Kauffman M. Development of the proteasome inhibitor Velcade (bortezomib). Cancer Invest 2004;22:304 – 11.

9. Fribley AM, Evenchik B, Zeng Q, et al. Proteasome inhibitor PS-341 induces apoptosis in cisplatin-resistant squamous cell carcinoma cells by induction of Noxa. J Biol Chem 2006;281:31440 – 7.

10. Fernandez Y, Verhaegen M, Miller TP, et al. Differential regulation of noxa in normal melanocytes and melanoma cells by proteasome inhibition: therapeutic implications. Cancer Res 2005;65:6294 – 304.

11. Yu C, Rahmani M, Dent P, Grant S. The hierarchical relationship between MAPK signaling and ROS generation in human leukemia cells undergoing apoptosis in response to the proteasome inhibitor bortezomib. Exp Cell Res 2004;295:555 – 66.

12. Lioni M, Brafford P, Andl C, et al. Dysregulation of claudin-7 leads to loss of E-cadherin expression and the increased invasion of esophageal squamous cell carcinoma cells. Am J Pathol 2007;170:709 – 21.

13. Velazquez OC, Snyder R, Liu ZJ, Fairman RM, Herlyn M. Fibroblast-dependent differentiation of human microvascular endothelial cells into capillary-like, three-dimensional networks. FASEB J 2002;16:1316 – 8.

14. Andl CD, Mizushima T, Nakagawa H, et al. Epidermal growth factor receptor mediates increased cell proliferation, migration, and aggregation in esophageal keratinocytes *in vitro* and *in vivo*. J Biol Chem 2003;278: 1824 – 30.

15. Haass NK, Sproesser K, Nguyen TK, et al. The mitogen-activated protein/extracellular signal-regulated kinase kinase inhibitor AZD6244 (ARRY-142886) induces growth arrest in melanoma cells and tumor regression when combined with docetaxel. Clin Cancer Res 2008;14: 230 – 9.

16. Smalley KS, Contractor R, Haass NK, et al. An organometallic protein kinase inhibitor pharmacologically activates p53 and induces apoptosis in human melanoma cells. Cancer Res 2007;67:209 – 17.

17. Barnas C, Martel-Planche G, Furukawa Y, Hollstein M, Montesano R, Hainaut P. Inactivation of the p53 protein in cell lines derived from human esophageal cancers. Int J Cancer 1997;71:79 – 87.

18. Lu C, Zhu F, Cho YY, et al. Cell apoptosis: requirement of H2AX in DNA ladder formation, but not for the activation of caspase-3. Mol Cell 2006;23:121 – 32.

19. Bulavin DV, Higashimoto Y, Popoff IJ, et al. Initiation of a G_2-M checkpoint after ultraviolet radiation requires p38 kinase. Nature 2001; 411:102 – 7.

20. Sunwoo JB, Chen Z, Dong G, et al. Novel proteasome inhibitor PS-341 inhibits activation of nuclear factor-κB, cell survival, tumor growth, and angiogenesis in squamous cell carcinoma. Clin Cancer Res 2001;7: 1419 – 28.

21. Allen C, Saigal K, Nottingham L, Arun P, Chen Z, Van Waes C. Bortezomib-induced apoptosis with limited clinical response is accompanied by inhibition of canonical but not alternative nuclear factor-κB subunits in head and neck cancer. Clin Cancer Res 2008;14: 4175 – 85.

22. Igarashi M, Dhar DK, Kubota H, Yamamoto A, El-Assal O, Nagasue N. The prognostic significance of microvessel density and thymidine phosphorylase expression in squamous cell carcinoma of the esophagus. Cancer 1998;82:1225 – 32.

23. Tanigawa N, Matsumura M, Amaya H, et al. Tumor vascularity correlates with the prognosis of patients with esophageal squamous cell carcinoma. Cancer 1997;79:220 – 5.

24. Kitadai Y, Amioka T, Haruma K, et al. Clinicopathological significance of vascular endothelial growth factor (VEGF)-C in human esophageal squamous cell carcinomas. Int J Cancer 2001;93:662 – 6.

25. el-Deiry WS, Tokino T, Velculescu VE, et al. WAF1, a potential mediator of p53 tumor suppression. Cell 1993;75:817 – 25.

26. Vousden KH, Prives C. p53 and prognosis: new insights and further complexity. Cell 2005;120:7 – 10.

27. Perez-Galan P, Roue G, Villamor N, Montserrat E, Campo E, Colomer D. The proteasome inhibitor bortezomib induces apoptosis in mantle-cell lymphoma through generation of ROS and Noxa activation independent of p53 status. Blood 2006;107:257 – 64.

28. Ling YH, Liebes L, Zou Y, Perez-Soler R. Reactive oxygen species generation and mitochondrial dysfunction in the apoptotic response to bortezomib, a novel proteasome inhibitor, in human H460 non-small cell lung cancer cells. J Biol Chem 2003;278:33714 – 23.

29. Cuadrado A, Lafarga V, Cheung PC, et al. A new p38 MAP kinase-regulated transcriptional coactivator that stimulates p53-dependent apoptosis. EMBO J 2007;26:2115 – 26.

30. Hideshima T, Richardson P, Chauhan D, et al. The proteasome inhibitor PS-341 inhibits growth, induces apoptosis, and overcomes drug resistance in human multiple myeloma cells. Cancer Res 2001;61: 3071 – 6.

31. Hideshima T, Podar K, Chauhan D, et al. p38 MAPK inhibition enhances PS-341 (bortezomib)-induced cytotoxicity against multiple myeloma cells. Oncogene 2004;23:8766 – 76.

32. Navas TA, Nguyen AN, Hideshima T, et al. Inhibition of p38α MAPK enhances proteasome inhibitor-induced apoptosis of myeloma cells by modulating Hsp27, Bcl-X(L), Mcl-1 and p53 levels *in vitro* and inhibits tumor growth *in vivo*. Leukemia 2006;20:1017 – 27.

Bortezomib induces apoptosis in esophageal squamous cell carcinoma cells through activation of the p38 mitogen-activated protein kinase pathway

Mercedes Lioni, Kazuhiro Noma, Andrew Snyder, et al.

Updated version	Access the most recent version of this article at: http://mct.aacrjournals.org/content/7/9/2866
Supplementary Material	Access the most recent supplemental material at: http://mct.aacrjournals.org/content/suppl/2008/09/05/7.9.2866.DC1

Cited articles	This article cites 31 articles, 12 of which you can access for free at: http://mct.aacrjournals.org/content/7/9/2866.full#ref-list-1
Citing articles	This article has been cited by 7 HighWire-hosted articles. Access the articles at: http://mct.aacrjournals.org/content/7/9/2866.full#related-urls

E-mail alerts	Sign up to receive free email-alerts related to this article or journal.
Reprints and Subscriptions	To order reprints of this article or to subscribe to the journal, contact the AACR Publications Department at pubs@aacr.org.
Permissions	To request permission to re-use all or part of this article, use this link http://mct.aacrjournals.org/content/7/9/2866. Click on "Request Permissions" which will take you to the Copyright Clearance Center's (CCC) Rightslink site.